J. Fluid Mech. (1985), *vol.* 156, *pp.* 151–166
Printed in Great Britain

The response of Helmholtz resonators to external excitation. Part 2. Arrays of slit resonators

By PETER A. MONKEWITZ

Department of Mechanical, Aerospace and Nuclear Engineering,
University of California at Los Angeles, CA 90024

(Received 29 June 1984)

The response of regular arrays of two-dimensional Helmholtz resonators mounted in a rigid baffle and subject to external excitation by a plane acoustic wave is studied. The inviscid linearized problem is solved by the matched-asymptotic-expansion technique in the low-frequency limit, i.e. when the characteristic neck dimension is small compared with the acoustic wavelength. Different spacings between resonators, from comparable with down to much smaller than the wavelength, as well as variable neck length and different cavity shapes, are studied without assumptions about the velocity distribution in the neck. The results yield predictions of resonance for the different geometries and compare favourably with measurements. Besides showing analytically the dependence, of, say, the acoustic impedance on all geometric parameters and forcing frequency, the analysis also reveals that for deep narrow cavities the basic Helmholtz model with uniform cavity pressure is inappropriate at resonance.

1. Introduction

In a first paper (Monkewitz & Nguyen-Vo 1985, subsequently referred to as [I]) single two- and three-dimensional resonators have been studied using singular perturbation techniques. The limit of long acoustic wavelength compared with the neck dimension was considered and the resonator cavity was scaled so as to keep the system tuned. For the cavity shapes considered in [I] with only one lengthscale, typified by semicylindrical and hemispherical cavities, it was shown that the basic Helmholtz spring–mass model applies to leading order, but that, for all practical purposes, improvements to the model are essential. By applying a rigorous matching procedure, any assumption on the velocity or pressure distribution in the neck to obtain the added neck length was avoided.

In this paper the analysis is extended to arrays of two-dimensional resonators mounted at regular intervals in an infinite rigid baffle. As the long-wavelength limit is considered, the problem can be broken up into subproblems associated with different regions: the outside wavefield, the neck region where the velocity field is essentially the same as for an incompressible fluid, and the cavity region. In §2 widely spaced resonators are considered, meaning that the distance between neighbouring resonators is taken to be of the same order as the wavelength. The neck and cavity geometry is taken directly from [I] (cf. figure 1). Therefore the solutions pertaining to these regions that were developed in [I] can be used and are referenced throughout the text with equation numbers preceded by I, e.g. (I1.1). Only the outside wavefield has to be modified to account for the interference between the resonators of the array. It is demonstrated that, in addition to the Helmholtz modes, the array can also be operated in an interference mode.

In §3 small spacings between resonators are considered. In order to have a physically realizable arrangement, the small spacing entails narrow cavities which have to be correspondingly deep for a resonance condition. These cavities with two lengthscales, as opposed to the one-lengthscale semicylindrical cavity, considerably complicate the analysis, as they require 'transition regions' between the neck and the outside wavefield as well as the cavity, where the waves, initially spreading radially from the orifice, are bent into plane waves. Apart from giving an asymptotically correct expression for the acoustic impedance, the calculation in the limit of vanishing ratio between neck width and wavelength yields the result that wave propagation in a 'two-lengthscale cavity' cannot be neglected. In fact it is shown that the larger dimension of the cavity approaches a quarter wavelength in the aforementioned limit.

Finally, the results are compared with theoretical and experimental results of Smits & Kosten (1951) who considered in the classical way both constant pressure and constant velocity at the resonator mouth to derive a lower and upper bound for the added length. Using a set of unpublished data of B. Walker, it is also shown that, say, the measured resonance frequency can be strongly dependent on the method of measurement. The present analysis thereby provides a tool to assess a measurement procedure and to compare results from different tests.

2. Widely spaced resonator arrays

In this section regularly spaced resonator arrays are considered with a spacing of the order of the acoustic wavelength. For simplicity the semicylindrical shape of the cavities used in [I] is maintained. Such an arrangement is physically realizable as long as the spacing is larger than a cavity diameter (cf. figure 1). Wide rectangular cavities, such as those considered by Smits & Kosten (1951), could be treated as well. It has to be remembered, though, that in order to obtain a rigorous asymptotic solution (in the limit of long wavelength) the expansions of the cavity solution near the neck for small r and the exterior Helmholtz solution for small r are required. Therefore, the approach of Smits & Kosten, to represent these solutions as Fourier series in y, is not practical, as it does not appear possible to determine their small-r behaviour analytically. Instead, the exterior solution is obtained directly in §3 by summing over an array of line sources. For rectangular cavities the summation would have to be extended over a two-dimensional source array with a period equal to the resonator spacing parallel to the baffle and a period equal to twice the cavity depth normal to the baffle. This poses no fundamental difficulty, but is somewhat awkward as, depending on the particular cavity dimension, the restrictions imposed on the use of the summation theorem for Bessel functions (see Gradshteyn & Ryzhik 1965, §8.53) will lead to different expressions for the solution.

In the following, the neck and cavity solutions derived in [I] are used without modification and matched to a new Helmholtz solution corresponding to an array of line sources.

2.1. *The Helmholtz region*

As in [I], all lengths in this region are made non-dimensional with the wavenumber $k = \omega/c_0$. For simplicity only normal incidence of the forcing plane wave is considered here. It is therefore described, together with its reflection from the baffle at $\hat{x} = \hat{b}$, where $\hat{x} = kx$, by

$$\hat{p} = \hat{p}_i \cos[\hat{x} - \hat{b}]. \tag{2.1}$$

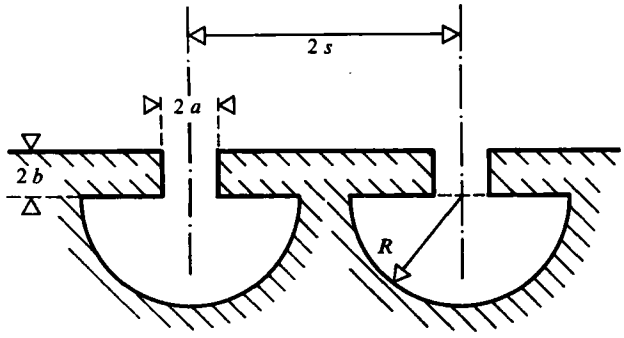

FIGURE 1. The geometry of the widely spaced arrays (see also figure 1 of [I]).

In contrast with the single resonator, the waves radiated from one slit are no longer simple cylindrical waves, but form a pattern, periodic in $\hat{y}$, with period $2\hat{s}$, the slit spacing. In the following it is assumed that $\hat{s}$ is of order unity, i.e. slit spacings comparable to the acoustic wavelength are considered. The appropriate solution of the Helmholtz equation

$$\hat{\nabla}^2\hat{p}+\hat{p}=0 \tag{2.2}$$

corresponding to an array of parallel line sources with spacing $2\hat{s}$ is given below. Owing to the assumed normal incidence of the forcing all sources are thereby in phase. As in [I], higher singularities such as dipoles and quadrupoles are not considered because they do not contribute to the flow rate through the slits and to the impedance up to the order in ϵ considered here. The required solution is

$$\hat{p}_0=\tfrac{1}{2}\mathrm{i}\pi\hat{A}_0\sum_{n=-\infty}^{+\infty}H_0^{(1)}[(4n^2\hat{s}^2+\hat{r}_0^2-4n\hat{s}\hat{r}_0\cos\theta_0)^{\frac{1}{2}}]. \tag{2.3}$$

For the matching of this solution to the neck solution developed in [I], the expansion of (2.3) for small radii $\hat{r}_0$ is required. Using expressions given in Gradshteyn & Ryzhik (1965, §8.52), and restricting attention to the case where the spacing $2\hat{s}$ is smaller than the acoustic wavelength, i.e. smaller than the first resonant spacing, one obtains

$$\left.\begin{aligned}\hat{p}_0&\approx\tfrac{1}{2}\mathrm{i}\pi\hat{A}_0\left\{H_0^{(1)}[\hat{r}_0]+2\sum_{n=1}^{\infty}H_0^{(1)}[2n\hat{s}]+O(\hat{r}_0^2)\right\}\\&\approx\hat{A}_0\left\{-\ln\hat{r}_0+\ln\frac{\hat{s}}{\pi}+\Delta\left(\frac{\hat{s}}{\pi}\right)+\frac{\mathrm{i}\pi}{2\hat{s}}+O(\hat{r}_0^2\ln\hat{r}_0)\right\}\end{aligned}\right\} \tag{2.4}$$

for $\hat{r}_0\to 0 \quad (0<\hat{s}<\pi)$;

$$\Delta(z)\equiv\sum_{n=1}^{\infty}\{(n^2-z^2)^{-\frac{1}{2}}-n^{-1}\}.$$

The lowest resonant spacing $\hat{s}=\pi$ corresponds to an inverse square-root singularity of the function Δ. For spacings larger than that, the expression for Δ has to be modified according to results in Gradshteyn & Ryzhik (1965), which poses no particular difficulty.

2.2. *Matching and results*

The solution in the neck region and in the semi-cylindrical cavity have already been developed in [I]. The only modification arises from the Helmholtz solution derived

above. With the intermediate scaling $x^* = \hat{x}\epsilon^{-\alpha}$ the expansion (I2.40) becomes now

$$\hat{p}_0 \approx \hat{p}_1 + \hat{A}_0(\epsilon)\left\{\alpha \ln\frac{1}{\epsilon} - \ln r_0^* + \ln\frac{\hat{s}}{\pi} + \Delta\left(\frac{\hat{s}}{\pi}\right) + \mathrm{i}\frac{\pi}{2\hat{s}} + O\left(\epsilon^{2\alpha}\ln\frac{1}{\epsilon}\right)\right\}. \tag{2.5}$$

With this and the unchanged expansion (I2.41) one obtains the following relations between amplitudes:

$$\left.\begin{aligned} \bar{A}_0 &= \hat{A}_0, \\ \bar{B}_0 &= \hat{p}_1 + \bar{A}_0\left\{\ln\frac{1}{\epsilon} + \ln\frac{\hat{s}}{\pi} + \Delta\left(\frac{\hat{s}}{\pi}\right) + \mathbb{D} + \frac{\mathrm{i}\pi}{2\hat{s}}\right\} \end{aligned}\right\} \tag{2.6}$$

The quantity $\mathbb{D}$ appearing here arose in [I], to which the reader is referred. These relations, which replace (I2.42), combined with (I2.45) immediately yield

$$\left.\begin{aligned} -\hat{p}_1\bar{A}_0^{-1} &= 2\ln\left(\frac{1}{\epsilon}\right)\left(1 - \frac{1}{\mu_0\bar{R}^2}\right) + \ln\frac{2\hat{s}}{\pi} + 2\mathbb{D} - \gamma + \Delta\left(\frac{\hat{s}}{\pi}\right) + \frac{\mathrm{i}\pi}{2\hat{s}} + O\left(\epsilon^2\ln^2\frac{1}{\epsilon}\right), \\ \bar{R} &= \hat{R}\left(\ln\frac{1}{\epsilon}\right)^{\frac{1}{2}}, \quad \mu_0 \equiv -\frac{4J_0'(\hat{R})}{\pi\hat{R}^2 Y_0'(\hat{R})} \end{aligned}\right\} \tag{2.7}$$

where $\gamma = 0.5772\ldots$ is the Euler constant. In (2.7), $\bar{R}$ is the rescaled cavity radius and μ_0 the volume correction factor found in [I] which accounts for the non-constant cavity pressure. Using the result (I2.25) for the average of the $\tilde{x}$-velocity over a resonator mouth area, the average over the entire baffle is obtained as

$$\bar{u} = \frac{\epsilon}{\hat{s}}\frac{\mathrm{i}\pi}{2\epsilon}\bar{A}_0 \tag{2.8}$$

with the area ratio factor $\epsilon/\hat{s}$. The impedance based on the incident pressure $\hat{p}_1$ and the average normal velocity $-\bar{u}$ on the baffle given by (2.8) then becomes

$$\bar{Z}_1 = -\frac{4\mathrm{i}\hat{s}}{\pi}\left\{\ln\left(\frac{1}{\epsilon}\right)\left(1 - \frac{1}{\mu_0\bar{R}^2}\right) + \tfrac{1}{2}\ln\frac{2\hat{s}}{\pi} + \mathbb{D} - \tfrac{1}{2}\gamma + \tfrac{1}{2}\Delta\left(\frac{\hat{s}}{\pi}\right)\right\} + 1. \tag{2.9}$$

The comparison with the basic spring–mass model

$$\bar{Z}_1 = \frac{\mathrm{i}S}{\ell V} - \mathrm{i}\ell\frac{S}{2a}[2b + l'] + \mathscr{R}, \tag{2.10}$$

where S is now the baffle area $2s$ per unit span associated with one resonator, finally yields the results

$$\left.\begin{aligned} V &= \tfrac{1}{2}\pi R^2\mu_0(\ell R), \\ \mathscr{R} &= 1, \\ \frac{l'}{a} &= \frac{4}{\pi}\left\{\ln\frac{1}{\ell a} + \frac{l''}{a}\right\} + \frac{2}{\pi}\frac{l'''}{a}, \\ \frac{l''}{a} &= \mathbb{D} - \frac{\pi b}{2a} + \ln 2 - \gamma, \\ \frac{l'''}{a} &= \ln\frac{\ell s}{2\pi} + \Delta\left(\frac{\ell s}{\pi}\right) + \gamma. \end{aligned}\right\} \tag{2.11}$$

The added length l' above is broken up into the single-resonator added length, a term which depends on the neck length, and a further term representing the interference between resonators. For approximate expressions for l''/a the reader is

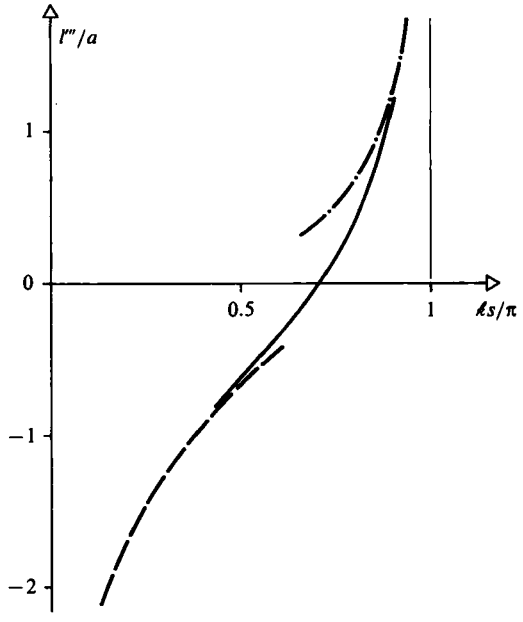

FIGURE 2. The contribution l'''/a to the added length dependent on the resonator spacing s: ——, $l'''/a \equiv \ln(ks/2\pi)+\gamma+\Delta(ks/\pi)$, with Δ defined by (2.4); – – –, $l'''/a \approx \ln(ks/2\pi)+\gamma+\frac{1}{2}(ks/\pi)^2\zeta(3)$ for $ks/\pi \to 0$; —·—, $l'''/a \approx [1-(ks/\pi)^2]^{-\frac{1}{2}}-1$ for $ks/\pi \to 1$.

referred to (I2.54) and (I2.55) and figure 5 of [I]. The following conclusions can now be drawn from these results.

(*a*) The effective volume or the stiffness of the system is the same as for a single resonator, and the reader is referred to the discussion in §2.4 of [I].

(*b*) At this order (neglecting terms of order ϵ^2) the interference between resonators of the array manifests itself in the added length $2l'''/\pi$ exclusively. It has to be reiterated here that in the derivation the spacing $2s$ has been assumed to be of the order of, but less than, a wavelength; taking the limit $s \to \infty$ to compare with the single-resonator results is therefore not possible.

The third term of l'/a in (2.11), namely the interference term l'''/a, shows a peculiar behaviour displayed in figure 2: for small spacings it is negative, i.e. the added length is reduced, while at a particular $ks = 0.7054\pi$ all interference effects cancel, and for $ks \to \pi$ the added length becomes infinite. The behaviour at small s can be understood by formally considering a spacing of the order of the neck width a, which is not realizable in practice because of the cavity geometry: it is immediately clear from (2.9) that the leading-order contribution $(4/\pi)\ln(1/\epsilon)$ to the added length is cut in half. This means that for small spacing the exterior wavefield does not contribute to the added length, which is not surprising as it consists of almost-plane waves all the way to the hydrodynamic near field of the resonator necks.

On the other hand, when $2s$ approaches a wavelength, or $\hat{s} \to \pi$, the added length becomes infinite, and with it the impedance. The reason for this behaviour is the approach of an interference resonance where the energy radiated by the resonators is no longer propagated away from the baffle, but 'piled up' in a transverse standing wave parallel to the baffle. This is most easily seen from a representation of the Helmholtz solution (2.3) in terms of a Fourier series in $\hat{y}$, as given by Smits & Kosten (1951) in their §4 (for $\hat{s} \to \pi$ their k_1 becomes zero). For non-normal incidence of the

forcing plane wave the situation becomes more complicated, however, because the resonators no longer operate in phase (cf. discussion at the end of this section).

(*c*) The resistance is identical with the resistance experienced by a piston radiating plane waves into a duct which can be thought of as being formed by the symmetry planes on both sides of each resonator.

The resonance condition for the lowest Helmholtz mode derived in [I], (I2.56), is now modified by interference to

$$\frac{1}{\mu_0 \hat{R}^2} = 1 + \frac{1}{2\ln(1/\epsilon)}\left(\ln\frac{2\hat{s}}{\pi} + 2\mathbb{D} - \gamma + \Delta\left(\frac{\hat{s}}{\pi}\right)\right). \tag{2.12}$$

As long as the interference is moderate or, in other words, the function Δ is of order unity, the scaling based on the balance between spring term and added-mass term associated with the cylindrical wavefield is appropriate, and will keep the system at resonance for $\epsilon \to 0$. If $\hat{s}$ approaches π, on the other hand, the resonant balance has to involve the spring term and Δ. Near $\hat{s} = \pi$ the function Δ can be approximated by

$$\left.\begin{aligned} \Delta\left(\frac{\hat{s}}{\pi}\right) &\approx (2\sigma)^{-\frac{1}{2}} + O(1), \\ \sigma &\equiv 1 - \frac{\hat{s}}{\pi} \ll 1. \end{aligned}\right\} \tag{2.13}$$

If now in (2.9) the function Δ dominates over the single-resonator added length of order $\ln(1/\epsilon)$, the proper resonant scaling becomes

$$\mu_0(\hat{R})\,\hat{R}^2 \approx 2(2\sigma)^{\frac{1}{2}}, \quad \sigma^{\frac{1}{2}} \ln\frac{1}{\epsilon} \ll 1. \tag{2.14}$$

This result provides quantitative guidance for designing sound-absorbing panels based on the interference resonance. In this mode the centre frequency is, to leading order, determined by the spacing of the resonators, while the sharpness of the resonance, which is of order σ, is determined by the cavity volume according to (2.14). The limitation on σ stated in (2.14) implies that the required cavities are much smaller than for the usual Helmholtz mode, while the resonance is sharper, which may be desirable for special applications.

It has to be noted, however, that the singularity of the function Δ depends on the angle of incidence of the forcing plane wave, which somewhat limits the possible applications of such a design. For oblique incidence at an angle φ between the wavevector and the baffle normal (cf. I2.5), a phase factor has to be added to the Helmholtz solution (2.3) representing an array of line sources:

$$\left.\begin{aligned} \hat{p}_0^{(\varphi)} &= \tfrac{1}{2}\mathrm{i}\pi\hat{A}_0 \sum_{n=-\infty}^{+\infty} \mathrm{e}^{2\mathrm{i}n\hat{s}\sin\varphi} H_0^{(1)}\left[(4n^2\hat{s}^2 + \hat{r}_0^2 - 4n\hat{s}\hat{r}_0\cos\theta)^{\frac{1}{2}}\right] \\ &\approx \hat{A}_0\left\{-\ln\hat{r}_0 + \ln\frac{\hat{s}}{\pi} + \Delta^{(\varphi)}\left(\frac{\hat{s}}{\pi}\right) + \frac{\mathrm{i}\pi}{2\hat{s}\cos\varphi} + O(\hat{r}_0^2\ln\hat{r}_0)\right\} \\ \text{for} \quad \hat{r}_0 &\to 0 \quad \left(0 < \hat{s} < \frac{\pi}{1+\sin\varphi}, \quad 0 \leqslant \varphi < \tfrac{1}{2}\pi\right), \end{aligned}\right\} \tag{2.15}$$

$$\Delta^{(\varphi)}(z) \equiv \sum_{n=1}^{\infty} \{\tfrac{1}{2}(n^2 - 2nz\sin\varphi - z^2\cos^2\varphi)^{-\frac{1}{2}} + \tfrac{1}{2}(n^2 + 2nz\sin\varphi - z^2\cos^2\varphi)^{-\frac{1}{2}} - n^{-1}\}.$$

Owing to the φ-dependence of the function Δ, the spacing for the interference mode can be generalized to $\hat{s}/\pi = 1/(1+\sin\varphi) - \sigma$ (cf. 2.13).

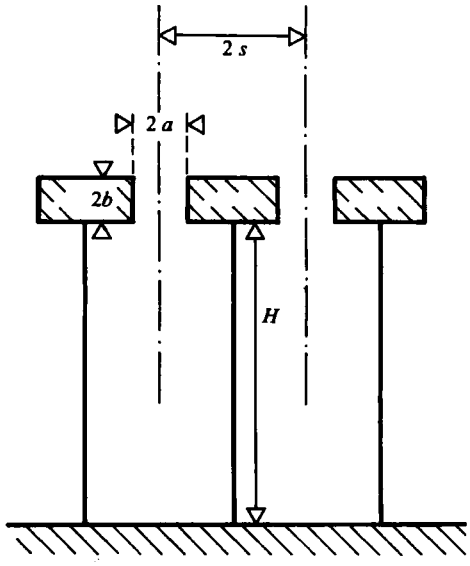

FIGURE 3. The geometry of the narrowly spaced arrays.

3. Closely spaced resonator arrays

In this section the most commonly used two-dimensional resonator arrays with a uniform spacing much smaller than the acoustic wavelength are analysed. In order to be physically realizable, the semicylindrical cavity has to be abandoned in favour of deep narrow cavities. To simplify matters, the width of the cavity is chosen to be the same as the resonator spacing $2s$, which is a geometry already considered by Smits & Kosten (1951) (cf. figure 3). In order to obtain rigorous results in the limit of very long wavelength compared with the slit width, the analysis has to include intermediate regions adjacent to the inside and outside of each resonator neck, where the transition from cylindrically spreading waves to plane waves further away from the neck takes place.

3.1. *The Helmholtz region*

As forcing, a plane wave, normally incident on the baffle, is again considered. Therefore the expression (2.1) can be used unchanged. The wave radiated by the resonators will, on the other hand, now also be plane outside the intermediate region mentioned above. It is thus described by

$$\hat{p}_0 = \hat{A}_0 \mathrm{e}^{\mathrm{i}\hat{x}}. \tag{3.1}$$

Periodic distortion (in the $\hat{y}$-direction) of this plane wave does not have to be considered, as it turns out to be exponentially small (see §3.2).

3.2. *The intermediate region*

In this subsection the wave equation is solved in the semi-infinite strip $x \geqslant 0, |y| \leqslant s$, with vanishing normal velocity on these 'boundaries' except for a source at the origin. At this point one can make use of the assumption that the resonator spacing $2s$ is much smaller than the wavelength but still much larger than the neck width $2a$. The coordinates in this region are thus rescaled according to

$$\check{x} = \frac{\hat{x}-b}{\epsilon^\beta}, \quad \check{y} = \frac{\hat{y}}{\epsilon^\beta}, \quad 0 < \beta < 1, \quad \check{s} = O(1). \tag{3.2}$$

This scaling implies that in the limit $\epsilon \to 0$ the ratio of open to total baffle area approaches zero like $\epsilon^{1-\beta}$. However, for situations with fixed neck geometry and slit pattern, where the wavelength is increased indefinitely to make ϵ go to zero, this ratio has to remain constant. This case requires that the spacing s be scaled in the same way as the neck dimensions a and b, and is discussed in §3.4 on results.

The Helmholtz equation equivalent to (I2.10) then becomes

$$\check{\nabla}^2 \check{p} = -\epsilon^{2\beta} \check{p}. \tag{3.3}$$

In complete analogy to [I], the solution is expanded in powers of $\epsilon^{2\beta}$ and satisfies the following equations:

$$\check{p}_n = \check{p}_{n,0} + \epsilon^{2\beta} \check{p}_{n,1} + \ldots, \tag{3.4a}$$

$$\check{\nabla}^2 \check{p}_{n,0} = 0, \quad \left.\frac{\partial \check{p}_{n,0}}{\partial \check{x}}\right|_{\check{x}=0} = 2\delta^{(n)}(\check{y}), \quad \left.\frac{\partial \check{p}_{n,0}}{\partial \check{y}}\right|_{\check{y}=\pm\check{s}} = 0, \tag{3.4b}$$

$$\check{\nabla}^2 \check{p}_{n,1} = -\check{p}_{n,0}, \quad \left.\frac{\partial \check{p}_{n,1}}{\partial \check{x}}\right|_{\check{x}=0} = \left.\frac{\partial \check{p}_{n,1}}{\partial \check{y}}\right|_{\check{y}=\pm\check{s}} = 0. \tag{3.4c}$$

The first index equal to n again indicates the leading behaviour of the solution: $n = 0, 1, 2, \ldots$ thereby correspond to a source, dipole, quadrupole etc. The leading-order hydrodynamic pressure corresponding to line sources at all the slits ($n = 0$), i.e. obeying (3.4b), has the same form as the potential of a row of point vortices, and can be taken from Lamb (1945 art. 156). It is given below, together with its Fourier-series representation, which is used subsequently:

$$\left.\begin{aligned} \check{p}_{0,0} &= \frac{\check{A}_0}{2}\left\{\ln\left[\cosh\frac{\pi\check{x}}{\check{s}} - \cos\frac{\pi\check{y}}{\check{s}}\right] - \ln 2\right\} + \check{B}_0 \\ &\equiv \check{A}_0\left\{\frac{\pi\check{x}}{2\check{s}} - \ln 2 - \sum_{n=1}^{\infty}\frac{1}{n}\,\mathrm{e}^{-n\pi\check{x}/\check{s}}\cos\left(\frac{n\pi\check{y}}{\check{s}}\right)\right\} + \check{B}_0, \end{aligned}\right\} \tag{3.5a}$$

$$\left.\begin{aligned} &\check{p}_{0,0} \propto \check{A}_0\left\{\frac{\pi\check{x}}{2\check{s}} - \ln 2\right\} + \check{B}_0 \quad (\check{x} \to \infty), \\ &\check{p}_{0,0} \approx \check{A}_0\left\{\ln\frac{\pi\check{r}_0}{2\check{s}} - \cos 2\theta_0\,\frac{1}{6}\left(\frac{\pi\check{r}_0}{2\check{s}}\right)^2 + O(\check{r}_0^4)\right\} + \check{B}_0 \quad (\check{r}_0 \to 0). \end{aligned}\right\} \tag{3.5b}$$

The large-$\check{x}$ and small-$\check{r}_0$ expansions are again listed for later use in the matching procedure. Proceeding to the solution of the Poisson equation (3.4c) for the next-order pressure $\check{p}_{0,1}$, one obtains in the Fourier representation

$$\check{p}_{0,1} = -\check{A}_0\left\{\frac{\check{x}^2}{2}\left(\frac{\pi\check{x}}{6\check{s}} - \ln 2\right) + \left(\frac{\check{s}}{\pi}\right)^2 \sum_{n=1}^{\infty}\frac{n\pi\check{x}+\check{s}}{2n^3\check{s}}\,\mathrm{e}^{-n\pi\check{x}/\check{s}}\cos\frac{n\pi\check{y}}{\check{s}}\right\} - \check{B}_0\frac{\check{x}^2}{2}, \tag{3.6a}$$

$$\check{p}_{0,1}(\check{x} = \check{y} = 0) = -\check{A}_0\left(\frac{\check{s}}{\pi}\right)^2\frac{\zeta(3)}{2}. \tag{3.6b}$$

The value of $\check{p}_{0,1}$ at the origin contains the Riemann zeta function of argument three, $\zeta(3) = 1.20206$. From the above, the expansion for large $\check{x}$ is just the zeroth Fourier coefficient, while for small $\check{r}_0$ the integration of the approximate form (3.5b) in polar coordinates, together with the result (3.6b), yields

$$\left.\begin{aligned} &\check{p}_{0,1} \propto -\frac{\check{x}^2}{2}\left\{\check{A}_0\left(\frac{\pi\check{x}}{6\check{s}} - \ln 2\right) + \check{B}_0\right\} + \ldots \quad (\check{x} \to \infty), \\ &\check{p}_{0,1} \approx -\check{A}_0\left\{\frac{\check{r}_0^2}{4}\left(\ln\frac{\pi\check{r}_0}{2\check{s}} - 1\right) + \left(\frac{\check{s}}{\pi}\right)^2\frac{\zeta(3)}{2}\right\} - \check{B}_0\frac{\check{r}_0^2}{4} + \ldots \quad (\check{r}_0 \to 0). \end{aligned}\right\} \tag{3.7}$$

The above results (3.7) will yield the leading-order correction of the impedance due to compressibility in the intermediate region. In order to include the leading-order correction due to the velocity-profile distortion in the neck by interference between resonators, the terms proportional to $\cos 2\theta$ have to be considered and matched as well.

The quadrupole solution of (3.4*b*) with $n = 2$ is simply obtained by taking the second x-derivative of the 'source' pressure (3.5). As such a solution is seen to decay exponentially away from the baffle, only its expansion near the resonator neck is required:

$$\check{p}_{2,0} \approx \check{A}_2 \left\{ \cos 2\theta_0 \left(\frac{2\check{s}}{\pi \check{r}_0}\right)^2 + \tfrac{1}{3} + \cos 2\theta_0 \frac{1}{15}\left(\frac{\pi \check{r}_0}{2\check{s}}\right)^2 + O(\cos 4\theta_0 \check{r}_0^4) \right\} \quad (\check{r}_0 \to 0). \tag{3.8}$$

Similarly, the solution behaving like an octupole at small $\check{r}_0$ is obtained from the fourth x-derivative of (3.5), and also contains $\cos 2\theta$ and constant terms, but it can be shown that this and higher multipole solutions only contribute to higher-order corrections to the impedance, which are not considered.

With this, the required solutions in the intermediate region are complete. It is understood that the same solutions can be used on the inside as well, to join the neck solution to the plane-wave solution in the narrow cavity. The only modification necessary is a redefinition of the $\check{x}$-coordinate to $\check{x} = -(\hat{x}+\hat{b})/\epsilon^\beta$.

For the neck, the solutions derived in [I] will be used without change. In addition, quadrupole solutions for the neck are derived in the Appendix in order to match the $\cos 2\theta$ terms. The only region left to be discussed is therefore the narrow rectangular cavity.

3.3. *The narrow cavity*

As seen from the intermediate solution (3.5) describing an array of sources, distortions of the plane wave die out exponentially away from the neck. It is therefore again sufficient to consider only plane waves in the cavity, of depth H, which is considered to be of the order of a wavelength. With the condition of vanishing velocity at $\bar{x} = \hat{H}$, one readily obtains

$$\bar{p}_0 = \bar{A}_0 \frac{\cos[\hat{H}-\bar{x}]}{\sin \hat{H}}, \quad \bar{x} = -(\hat{b}+\hat{x}), \tag{3.9a}$$

$$\bar{p}_0 \approx \bar{A}_0 \left\{ \vartheta_0(\hat{H})\, h(1-\beta)\, \epsilon^\beta \ln\left(\frac{1}{\epsilon}\right)(1-\tfrac{1}{2}\bar{x}^2) + \bar{x} - \tfrac{1}{6}\bar{x}^3 + O(\bar{x}^4) \right\} \quad (\bar{x} \to 0), \tag{3.9b}$$

$$\vartheta_0(z) \equiv \frac{\cot z}{\frac{1}{2}\pi - z}, \quad h(1-\beta)\,\epsilon^\beta \ln\frac{1}{\epsilon} \equiv \tfrac{1}{2}\pi - \hat{H}.$$

The definition of the function ϑ_0 and the scaling of h is left for later discussion. It is only noted here that for $\hat{H} \to \frac{1}{2}\pi$, or in other words $\epsilon \to 0$ while $h = O(1)$, the function ϑ_0 approaches unity.

3.4. *Results*

The tedious matching procedure is outlined and partly carried out in detail in the Appendix. To determine the impedance of the resonator array, one only needs the final result (A 17). Again using (2.8) with the area ratio $\epsilon/\hat{s} = \epsilon^{1-\beta}/\check{s}$, the impedance based on the normal velocity averaged over the entire panel is obtained as

$$\bar{Z}_1 = \frac{4\mathrm{i}\epsilon^\beta \check{s}}{\pi}\left\{(1-\beta)\ln\left(\frac{1}{\epsilon}\right)\left(\frac{\pi h \vartheta_0(\hat{H})}{4\check{s}} - 1\right) + \ln\frac{\pi}{\check{s}} - \mathbb{D} - \epsilon^{2\beta}\frac{\zeta(3)\,\check{s}^2}{2\pi^2} \right.$$
$$\left. - \epsilon^{2-2\beta}\frac{1+k^2}{3D^2}\left(\frac{\pi}{2\check{s}}\right)^2 + O(\epsilon^{4\beta}, \epsilon^2, \epsilon^{4-4\beta})\right\} + 1, \tag{3.10}$$

with k and D defined by (I2.13) and (I2.14). The main difference from the previous case with the semicircular cavity lies in the spring term, which, after removing all the scaling (cf. 3.9*b*), has the simple form also found by Smits & Kosten (1951) and Panton & Miller (1975):

$$(1-\beta)\,\epsilon^{\beta}\ln\left(\frac{1}{\epsilon}\right)h\vartheta_0(\hat{H}) = \cot(\ell H). \tag{3.11}$$

The radiation resistance is unchanged and equal to unity (times $\rho_0 c_0$) and the added length l' (see (2.10)) is

$$\frac{l'}{a} = \frac{4}{\pi}\left\{\ln\frac{s}{2\pi a}+\frac{l''}{a}+\gamma+\frac{\zeta(3)\,(\ell s)^2}{2\pi^2}+\frac{1+k^2}{3D^2}\left(\frac{\pi a}{2s}\right)^2\right\}. \tag{3.12}$$

For the definition of l'' see (2.11) and also figure 5 of [I].

The main results of this analysis are the following.

(*a*) The spring term (3.11), although already derived by other authors cited above, needs to be reinterpreted. So far the result (3.11) has been thought to confirm the basic Helmholtz model with a cavity of essentially uniform pressure. By expanding the cotangent for small argument it can indeed be pressed into the standard form:

$$\mathrm{i}\cot\ell H \approx \frac{\mathrm{i}\,2s}{\ell H\,2s} = \frac{\mathrm{i}S}{\ell V}. \tag{3.13}$$

This interpretation turns out to be inconsistent with the long-wavelength assumption and the condition that the resonator be tuned.

The use of the matched-asymptotic-expansion technique involving the limit process $\epsilon\to 0$ reveals that in this limit the length of the narrow cavity has to approach a quarter wavelength for the system to stay tuned, i.e. for the reactance to stay zero. The manner in which the quarter-wave cavity is approached is determined by the scaling of h (cf. 3.9*b*). It is now justified a posteriori by the balance in (3.10) between the spring and the leading-order mass term which leads to the following resonance condition (to leading order independent of ϵ, as it should be):

$$\frac{\pi h\vartheta_0[\hat{H}]}{4\check{s}} = 1-\frac{1}{(1-\beta)\ln(1/\epsilon)}\left\{\ln\frac{\pi}{\check{s}}-\mathbb{D}-\epsilon^{2\beta}\frac{\zeta(3)\,\check{s}^2}{2\pi^2}-\epsilon^{2-2\beta}\frac{1+k^2}{3D^2}\left(\frac{\pi}{2\check{s}}\right)^2\right\}. \tag{3.14}$$

This shows that tuned resonators with narrow deep cavities do not operate according to the basic Helmholtz model, and never approach the mode of operation with uniform cavity pressure, not even in the limit of an infinite ratio between wavelength and neck width!

(*b*) As already mentioned earlier, and also in [I], the leading-order added length $(4/\pi)\ln(1/\epsilon)$ of the single resonator or widely spaced resonators is reduced by a factor $1-\beta$ owing to the confinement of the wavefield into a 'channel' of half-width $\ell s = \epsilon^{\beta}\check{s}$, $\check{s} = O(1)$. In addition, the added length is again determined together with specific error bounds without recourse to any assumptions about the velocity or pressure distribution in the neck exit plane.

(*c*) The added-length term proportional to $\epsilon^{2-2\beta}$, which is related to the distortion of the velocity profile in the mouth plane due to neighbouring resonators, obviously becomes more important if the spacing is reduced relative to the slit width, or, in other words, if β approaches 1. In the limiting case where the ratio of open to total baffle area is required to stay constant as $\epsilon\to 0$, the expansion (3.10) for the impedance breaks down. The procedure to follow then is to find a new conformal mapping of

the neck *and* the adjacent intermediate regions onto a half-plane, which implies that the neck dimensions a, b and the half-spacing s all be of the same order, namely $O(\epsilon)$. This is not carried out, as the result for a neck of zero length can be readily obtained from Morse & Ingard (1968, §9.1), where they treat the transmission of plane waves through a two-dimensional channel with a finlike obstruction. By matching their result for the hydrodynamic near field to the Helmholtz region and to the narrow-cavity solution (3.9), the impedance corresponding to (3.10) is found to be

$$\bar{Z}_i(\tilde{b}=0) = \mathrm{i}\cot\hat{H} - \frac{4\mathrm{i}\epsilon\tilde{s}}{\pi}\ln\left(\frac{1}{2q}+\frac{q}{2}\right)+1+O(\epsilon^3), \tag{3.15}$$

$$q = \tan\frac{\pi\tilde{a}}{4\tilde{s}}, \quad \tilde{s} = O(1).$$

Upon expanding for small ratios $\tilde{a}/\tilde{s}$, one obtains for the second term, the mass term, in (3.15)

$$-\frac{4\mathrm{i}\epsilon\tilde{s}}{\pi}\ln\left(\frac{1}{2q}+\frac{q}{2}\right) \approx -\frac{4\mathrm{i}\epsilon\tilde{s}}{\pi}\left\{\ln\frac{2\tilde{s}}{\pi\tilde{a}}+\frac{1}{6}\left(\frac{\pi\tilde{a}}{2\tilde{s}}\right)^2+\frac{1}{180}\left(\frac{\pi\tilde{a}}{2\tilde{s}}\right)^4+\ldots\right\} \quad \left(\frac{\tilde{a}}{\tilde{s}}\to 0\right). \tag{3.16}$$

Recalling from (I 2.23) that for $\tilde{b}=0$ the parameters k and D take on the values $k=1$ and $D=2$, one recovers exactly the term proportional to $\epsilon^{2-2\beta}$ in (3.10). What has been gained from the present analysis is the detailed dependence of this term on the neck length, which is vital for accurate resonance prediction. It is seen from (I 2.24) that the coefficient $(1+k^2)/3D^2$ changes considerably, from $\frac{1}{6}$ for $\tilde{b}=0$ to 0.135 for long necks. In addition, comparison of (3.10) with the expansion (3.16) shows that the next term in the impedance, proportional to $\epsilon^{4-4\beta}$, is negligible for all practical purposes owing to its very small coefficient. Finally the conclusions regarding the resonance condition are also fully confirmed for $\beta=1$: from (3.15) it is clear that $\hat{H}$ has to be equal to $\frac{1}{2}\pi$, a quarter-wavelength, minus an amount of order ϵ to balance the mass term. Consequently, when $\beta=1$, only the scaling factor $(1-\beta)\ln(1/\epsilon)$ has to be removed from the definition (3.9a) of h.

4. Comparison with experiments, and conclusions

The results obtained from linear inviscid theory are now compared with measurements by Smits & Kosten (1951) and by B. Walker (unpublished private communication). The first set of data were obtained in an interferometer tube, and correspond to the truly two-dimensional geometry of figure 3. Walker's data, on the other hand, were obtained with only six resonators of 47 cm span, arranged as in figure 3. The far field in his arrangement was therefore three-dimensional. Also, his method of determining the resonance frequency consisted of driving the cavity with a speaker operating at constant displacement amplitude and searching for the maximum pressure amplitude in the cavity. In order to analyse this case, one has to add a driving term to (3.9a): to simplify matters, the whole cavity bottom at $\bar{x}=\hat{H}$ is assumed to oscillate with a velocity amplitude $\bar{u}_b$. Equation (3.9) is therefore modified to

$$\bar{p}_0 = \bar{A}_0\frac{\cos(\hat{H}-\bar{x})}{\sin\hat{H}}+\bar{u}_b\frac{\cos\bar{x}}{\sin\hat{H}}, \tag{4.1a}$$

$$\bar{p}_0 \approx \bar{A}_0\{\cot\hat{H}+\bar{x}\}+\frac{\bar{u}_b}{\sin\hat{H}}+O(\bar{x}^2) \quad \text{as } \bar{x}\to 0. \tag{4.1b}$$

Case	a (mm)	b (mm)	s (mm)	H (mm)	Source
1	3.64	2	114	72.8	Smits & Kosten (1951)
2	3.64	2	114	54.6	
3	3.64	2	114	7.3	
4	12.7	19	57	413	B. Walker (private communication)
5	12.7	1	57	413	

TABLE 1. Geometrical data of experiments

Case	Measured centre frequency (Hz)	'Wide spacing' (2.12) (Hz)	'Narrow spacing' (3.14) (Hz)	$\frac{\partial \lvert \bar{p}_0(\bar{x}=\hat{H}) \rvert}{\partial k} = 0$ (4.1) (Hz)
1	263	261	260	—
2	320	304	301	—
3	625	—	—	—
4	113	152	133	112
5	125	220	170	126

TABLE 2. Comparison of measured and calculated resonance frequencies using $c_0 = 340$ m/s

Using (4.1a) instead of (A 15b) in the Appendix and switching off the external forcing $\hat{p}_i$ in (A 13a) leads in a straightforward manner to the amplitude $\bar{A}_0$ in the cavity as

$$\bar{A}_0 = -\frac{\bar{u}_b}{\sin \hat{H}} \frac{\pi}{4\epsilon^\beta \check{s}} \left\{ \frac{\pi \cot \hat{H}}{4\epsilon^\beta \check{s}} - (1-\beta) \ln \frac{1}{\epsilon} + \ln \frac{\pi}{\check{s}} - \mathbb{D} - \epsilon^{2\beta} \frac{\zeta(3)}{2} \left(\frac{\check{s}}{\pi}\right)^2 - \epsilon^{2-2\beta} \frac{1+k^2}{3D^2} \left(\frac{\pi}{2\check{s}}\right)^2 - \frac{i\pi}{4\epsilon^\beta \check{s}} \right\}^{-1}. \quad (4.2)$$

With the result (4.2) one can now find the wavenumber k that maximizes the pressure amplitude $|\bar{p}_0|$ in the cavity at, say, the bottom wall $\bar{x} = \hat{H}$.

In the following, the geometrical data for the different measurements are given in table 1. In table 2 the measured resonance frequencies are compared with the predictions for widely and narrowly spaced arrays. The comparison with the first result (2.12) is thereby based on a semicylindrical cavity of equal volume. In the first two cases all predictions, including Smits & Kosten's, are within the experimental error. The third case of the wide shallow cavity is included to illustrate the point being made regarding the rigorous long-wavelength limit. For this purpose, the shallow cavity can be viewed qualitatively as a deep narrow cavity split down the middle and folded up along the baffle. Its depth is thereby equal to 114 mm (the half-spacing s), and does indeed approach a quarter-wavelength, which is 136 mm at the measured resonance frequency of 625 Hz.

In the last two cases, 4 and 5, finally, the resonance condition (2.12) does not give good results because, as noted earlier, the cavities have proportions very different from semicylindrical. The condition (3.14) for narrow spacing, on the other hand, is expected to predict the resonance accurately This claim is substantiated by the result obtained from maximizing $|\bar{p}_0(\bar{x} = \hat{H})|$ (cf. (4.1)), which is based on the same linearized

inviscid analysis. The extremely close agreement with measured frequencies is thereby somewhat fortuitous, as the speed of sound was not accurately recorded during the experiments; notwithstanding this, the ratio of the frequencies for cases 4 and 5 is predicted to within 1.7%. These last results demonstrate convincingly that the method of resonance-frequency measurement does have a significant influence on the result, which is not expected on the basis of the simple Helmholtz model with uniform cavity pressure.

In summary, different types of two-dimensional resonator arrays have been analysed, relying entirely on a singular perturbation approach. The results, which are exact in the long-wavelength limit, allow the prediction of resonance for widely and narrowly spaced arrays, arbitrary neck length and different modes without recourse to assumptions on the velocity distribution in the neck. For the case of narrowly spaced arrays which entail narrow deep cavities it is shown that even in the long-wavelength limit it is not permissible to model the cavity as a volume of uniform pressure. In fact it is demonstrated that in this limit the cavity depth has to approach a quarter-wavelength for resonance. This conclusion is of course also valid for a single resonator with a deep narrow cavity. The analysis of this paper finally permits one to assess measurement procedures for the response frequency of resonators, such as two-microphone methods and cavity excitation, for instance.

The author wishes to thank Dr B. Walker and Dr L. W. Sepmeyer for the ready access to their data and the helpful discussions.

Appendix. Matching procedure for the closely spaced resonator array

In the following, the $\cos 2\theta$ terms are matched first, because the 'quadrupole' solutions also contribute constants to the matching of 'source' solutions. To do this, quadrupole solutions in the neck region have to be developed. Using results obtained in [I], the complex potential

$$F_2^{(\pm)} = w^{\pm 2} \tag{A 1}$$

is considered. In order to obtain the asymptotic expansions on both sides of the neck, the asymptotic form (I2.18) of the conformal mapping between the physical z-plane and w has to be carried to higher order:

$$z - b \approx -\frac{\mathrm{i}}{D}\left\{\frac{k}{w} + \frac{1+k^2}{2}\frac{w}{k} + \frac{(1-k^2)^2}{24}\left(\frac{w}{k}\right)^3 + O(|w|^5)\right\} \quad (|w| \to 0). \tag{A 2}$$

Using (I2.17) and (A 2) the asymptotic expansions of the real part of F are obtained as

$$\left.\begin{aligned}
&\tilde{p}_{2,0}^{(+)} \propto \tilde{A}_2^{(+)}\left\{\cos 2\theta_0 \frac{k^2}{D^2\tilde{r}_0^2} + O\left(\frac{\cos 4\theta_0}{\tilde{r}_0^4}\right)\right\}, \\
&\tilde{p}_{2,0}^{(-)} \propto \tilde{A}_2^{(-)}\left\{\cos 2\theta_0 \frac{D^2\tilde{r}_0^2}{k^2} - \frac{1+k^2}{k^2} - \cos 2\theta_0 \frac{1+k^2+k^4}{3(kD\tilde{r}_0)^2} + O\left(\frac{\cos 4\theta_0}{\tilde{r}_0^4}\right)\right\}
\end{aligned}\right\} \quad (\tilde{r}_0 \to \infty),$$

$$\left.\begin{aligned}
&\tilde{p}_{2,0}^{(+)} \propto \tilde{A}_2^{(+)}\left\{\cos 2\theta_\mathrm{i} D^2\tilde{r}_\mathrm{i}^2 - (1+k^2) - \cos 2\theta_\mathrm{i} \frac{1+k^2+k^4}{3(D\tilde{r}_\mathrm{i})^2} + O\left(\frac{\cos 4\theta_\mathrm{i}}{\tilde{r}_\mathrm{i}^4}\right)\right\}, \\
&\tilde{p}_{2,0}^{(-)} \propto \tilde{A}_2^{(-)}\left\{\cos 2\theta_\mathrm{i} \frac{1}{D^2\tilde{r}_\mathrm{i}^2} + O\left(\frac{\cos 4\theta_\mathrm{i}}{\tilde{r}_\mathrm{i}^4}\right)\right\}
\end{aligned}\right\} \quad (\tilde{r}_\mathrm{i} \to \infty). \tag{A 3}$$

The quantities D and k are defined by (I2.13) and (I2.14) in [I], where also useful approximations are given by (I2.23) and (I2.24). As noted earlier, the source-type solutions also contribute terms proportional to $\cos 2\theta$, as evidenced by (3.5b) for the intermediate region and by (I2.20) for the neck region. For the present purpose, the $\cos 2\theta$ term has to be included in the asymptotic expansions (I2.22) of the source solution in the neck to yield

$$\left.\begin{aligned}\tilde{p}_{0,0} &\propto -\tilde{A}_0\left\{\ln\tilde{r}_0+\mathbb{D}-\cos 2\theta_0\,\frac{1+k^2}{2(D\tilde{r}_0)^2}+\ldots\right\} \quad (\tilde{r}_0\to\infty),\\ \tilde{p}_{0,0} &\propto +\tilde{A}_0\left\{\ln\tilde{r}_i+\mathbb{D}-\cos 2\theta_i\,\frac{1+k^2}{2(D\tilde{r}_i)^2}+\ldots\right\} \quad (\tilde{r}_i\to\infty).\end{aligned}\right\} \tag{A 4}$$

Now the terms proportional to $\cos 2\theta$ can be collected in all relevant solutions of the neck and adjacent intermediate regions on the outside (0) and on the inside (i). On the outside one obtains the following expansions of the $\cos[2\theta]$ terms for small $\check{r}_0$ and large $\tilde{r}_0$:

$$\left.\begin{aligned}\check{p}^{(0)} &\approx \ldots+\cos 2\theta_0\left\{\hat{p}_i\frac{\check{r}_0^2}{4}-\check{A}_0^{(0)}\,\frac{1}{6}\left(\frac{\pi\check{r}_0}{2\check{s}}\right)^2+\check{A}_2^{(0)}\left[\left(\frac{2\check{s}}{\pi\check{r}_0}\right)^2+\frac{1}{15}\left(\frac{\pi\check{r}_0}{2\check{s}}\right)^2\right]\right\} \quad (\check{r}_0\to 0),\\ \tilde{p} &\propto \ldots+\cos 2\theta_0\left\{\tilde{A}_0\frac{1+k^2}{2(D\tilde{r}_0)^2}+\tilde{A}_2^{(+)}\left(\frac{k}{D\tilde{r}_0}\right)^2+\tilde{A}_2^{(-)}\left[\left(\frac{D\tilde{r}_0}{k}\right)^2-\frac{1+k^2+k^4}{3(kD\tilde{r}_0)^2}\right]\right\} \quad (\tilde{r}_0\to\infty).\end{aligned}\right\} \tag{A 5}$$

Similarly one obtains on the inside

$$\left.\begin{aligned}\tilde{p} &\propto \ldots+\cos 2\theta_i\left\{-\tilde{A}_0\frac{1+k^2}{2(D\tilde{r}_i)^2}+\tilde{A}_2^{(-)}(D\tilde{r}_i)^{-2}+\tilde{A}_2^{(+)}\left[(D\tilde{r}_i)^2-\frac{1+k^2+k^4}{3(D\tilde{r}_i)^2}\right]\right\} \quad (\tilde{r}_i\to\infty),\\ \check{p}^{(i)} &\approx \ldots+\cos 2\theta_i\left\{-\check{A}_0^{(i)}\,\frac{1}{6}\left(\frac{\pi\check{r}_i}{2\check{s}}\right)^2+\check{A}_2^{(i)}\left[\left(\frac{2\check{s}}{\pi\check{r}_i}\right)^2+\frac{1}{15}\left(\frac{\pi\check{r}_i}{2\check{s}}\right)^2\right]\right\} \quad (\check{r}_i\to 0).\end{aligned}\right\} \tag{A 6}$$

In the above expressions it is understood that all amplitudes are functions of ϵ. Now, the intermediate matching procedure (Kevorkian & Cole 1981) can be applied by rescaling according to

$$\begin{aligned} r^* &= \epsilon^{-\alpha}\hat{r}, \quad \beta<\alpha<1, \\ \tilde{r} &= \epsilon^{\alpha-1}r^*, \quad \check{r}=\epsilon^{\alpha-\beta}r^*. \end{aligned} \tag{A 7}$$

Introducing this scaling into (A 5) and (A 6) and equating the outside and inside pairs of solutions in the overlap domain, one obtains

$$\begin{aligned} &r_0^{*2}\left\{\epsilon^{2\alpha}\frac{\hat{p}_i}{4}-\epsilon^{2\alpha-2\beta}\check{A}_0^{(0)}\,\frac{1}{6}\left(\frac{\pi}{2\check{s}}\right)^2+\epsilon^{2\alpha-2\beta}\check{A}_2^{(0)}\,\frac{1}{15}\left(\frac{\pi}{2\check{s}}\right)^2\right\}+\frac{1}{r_0^{*2}}\epsilon^{2\beta-2\alpha}\check{A}_2^{(0)}\left(\frac{2\check{s}}{\pi}\right)^2 \\ &\qquad = r_0^{*2}\epsilon^{2\alpha-2}\tilde{A}_2^{(-)}\frac{D^2}{k^2}+\frac{1}{r_0^{*2}}\epsilon^{2-2\alpha}\left\{\tilde{A}_0\frac{1+k^2}{2D^2}+\tilde{A}_2^{(+)}\frac{k^2}{D^2}-\tilde{A}_2^{(-)}\frac{1+k^2+k^4}{3(kD)^2}\right\}, \end{aligned} \tag{A 8}$$

$$\begin{aligned} &r_i^{*2}\epsilon^{2\alpha-2}\tilde{A}_2^{(+)}D^2+\frac{1}{r_i^{*2}}\epsilon^{2-2\alpha}\left\{-\tilde{A}_0\frac{1+k^2}{2D^2}-\tilde{A}_2^{(+)}\frac{1+k^2+k^4}{3D^2}+\tilde{A}_2^{(-)}D^{-2}\right\} \\ &\qquad = r_i^{*2}\epsilon^{2\alpha-2\beta}\left\{-\check{A}_0^{(i)}\,\frac{1}{6}\left(\frac{\pi}{2\check{s}}\right)^2+\check{A}_2^{(i)}\,\frac{1}{15}\left(\frac{\pi}{2\check{s}}\right)^2\right\}+\frac{1}{r_i^{*2}}\epsilon^{2\beta-2\alpha}\check{A}_2^{(i)}\left(\frac{2\check{s}}{\pi}\right)^2. \end{aligned} \tag{A 9}$$

In order to solve the above equations for the quadrupole amplitudes, one has to use the leading-order results for the source amplitudes $\check{A}_0^{(0)}$, $\tilde{A}_0$ and $\check{A}_0^{(i)}$, which are derived later on to avoid dealing with the source terms twice. As it will turn out, all these amplitudes are, up to logarithmic factors $\ln(1/\epsilon)$, of the same order as the incident pressure $\hat{p}_i$. Therefore, the quadrupole amplitudes are to leading order (independent of r^* and α!) given by

$$\left.\begin{aligned} \check{A}_2^{(0)} &= \epsilon^{2-2\beta}\tilde{A}_0\frac{1+k^2}{2D^2}\left(\frac{\pi}{2\check{s}}\right)^2, \quad \tilde{A}_2^{(-)} = -\epsilon^{2-2\beta}\check{A}_0^{(0)}\frac{k^2}{6D^2}\left(\frac{\pi}{2\check{s}}\right)^2, \\ \tilde{A}_2^{(+)} &= -\epsilon^{2-2\beta}\check{A}_0^{(i)}\frac{1}{6D^2}\left(\frac{\pi}{2\check{s}}\right)^2, \quad \check{A}_2^{(i)} = -\epsilon^{2-2\beta}\tilde{A}_0\frac{1+k^2}{2D^2}\left(\frac{\pi}{2\check{s}}\right)^2. \end{aligned}\right\} \tag{A 10}$$

At this point the matching of the source solutions including the leading-order effect of their quadrupole distortions can be performed by noting that, according to (3.8), (A 3) and (A 4), the quadrupole solutions contribute the following constants of order $\epsilon^{2-2\beta}$ to be added to the source solutions:

$$\left.\begin{aligned} &\text{outside intermediate region } (\check{r}_0\to 0): && \tfrac{1}{3}\check{A}_2^{(0)}, \\ &\text{outside neck region} && (\tilde{r}_0\to\infty): \quad -\frac{1+k^2}{k^2}\tilde{A}_2^{(-)}, \\ &\text{inside neck region} && (\tilde{r}_i\to\infty): \quad -(1+k^2)\,\tilde{A}_2^{(+)}, \\ &\text{inside intermediate region} && (\check{r}_i\to 0): \quad \tfrac{1}{3}\check{A}_2^{(i)}. \end{aligned}\right\} \tag{A 11}$$

The expansions of the θ-independent terms in all regions, including the above constants, are summarized below.

Helmholtz region (radiated plane wave (3.1) only):

$$\hat{p}_0 \approx \hat{A}_0\{1+\mathrm{i}\hat{x}-\tfrac{1}{2}\hat{x}^2+\ldots\} \quad (\hat{x}\to 0). \tag{A 12a}$$

Outside intermediate region (cf. (3.5*b*) and (3.7)):

$$\check{p}_0^{(0)} \propto \check{A}_0^{(0)}\left\{\frac{\pi\check{x}}{2\check{s}}-\ln 2-\epsilon^{2\beta}\left[\frac{\pi\check{x}^3}{12\check{s}}-\frac{\check{x}^2}{2}\ln 2\right]\right\}+\check{B}_0^{(0)}\left\{1-\epsilon^{2\beta}\frac{\check{x}^2}{2}\right\} \quad (\check{x}\to\infty), \tag{A 12b}$$

$$\check{p}_0^{(0)} \approx \hat{p}_i\{1-\tfrac{1}{4}\hat{r}_0^2\}+\check{A}_0^{(0)}\left\{\ln\frac{\pi\check{r}_0}{2\check{s}}-\epsilon^{2\beta}\left[\frac{\zeta(3)}{2}\left(\frac{\check{s}}{\pi}\right)^2+\frac{\check{r}_0^2}{4}\left(\ln\frac{\pi\check{r}_0}{2\check{s}}-1\right)\right]\right\}$$
$$+\check{B}_0^{(0)}\left\{1-\epsilon^{2\beta}\frac{\check{r}_0^2}{4}\right\}+\epsilon^{2-2\beta}\tilde{A}_0\frac{1+k^2}{6D^2}\left(\frac{\pi}{2\check{s}}\right)^2 \quad (\check{r}_0\to 0). \tag{A 13a}$$

Outside neck region (cf. (I2.22) and (I2.29)):

$$\tilde{p}_0 \propto -\tilde{A}_0\left\{\ln\tilde{r}_0+\mathbb{D}-\epsilon^2\frac{\tilde{r}_0^2}{4}[\ln\tilde{r}_0+\mathbb{D}-1]\right\}+\tilde{B}_0\left\{1-\epsilon^2\frac{\tilde{r}_0^2}{4}\right\}+\epsilon^{2-2\beta}\check{A}_0^{(0)}\frac{1+k^2}{6D^2}\left(\frac{\pi}{2\check{s}}\right)^2$$
$$(\tilde{r}_0\to\infty). \tag{A 13b}$$

Inside neck region:

$$\tilde{p}_0 \propto +\tilde{A}_0\left\{\ln\tilde{r}_i+\mathbb{D}-\epsilon^2\frac{\tilde{r}_i^2}{4}[\ln\tilde{r}_i+\mathbb{D}-1]\right\}+\tilde{B}_0\left\{1-\epsilon^2\left[\frac{\tilde{r}_i^2}{4}+\frac{4b}{\pi}\ln\tilde{r}_i\right]\right\}$$
$$+\epsilon^{2-2\beta}\check{A}_0^{(i)}\frac{1+k^2}{6D^2}\left(\frac{\pi}{2\check{s}}\right)^2 \quad (\tilde{r}_i\to\infty). \tag{A 14a}$$

Inside intermediate region (cf. (3.5b) and (3.7)):

$$\check{p}_0^{(i)} \approx \check{A}_0^{(i)}\left\{\ln\frac{\pi\check{r}_i}{2\check{s}}-\epsilon^{2\beta}\left[\frac{\zeta(3)}{2}\left(\frac{\check{s}}{\pi}\right)^2+\frac{\check{r}_i^2}{4}\left(\ln\frac{\pi\check{r}_i}{2\check{s}}-1\right)\right]\right\}$$
$$+\check{B}_0^{(i)}\left\{1-\epsilon^{2\beta}\frac{\check{r}_i^2}{4}\right\}-\epsilon^{2-2\beta}\tilde{A}_0\frac{1+k^2}{6D^2}\left(\frac{\pi}{2\check{s}}\right)^2 \quad (\check{r}_i\to 0), \quad \text{(A 14}b\text{)}$$

$$\check{p}_0^{(i)} \propto \check{A}_0^{(i)}\left\{\frac{\pi\check{x}}{2\check{s}}-\ln 2-\epsilon^{2\beta}\left[\frac{\pi\check{x}^3}{12\check{s}}-\frac{\check{x}^2}{2}\ln 2\right]\right\}+\check{B}_0^{(i)}\left\{1-\epsilon^{2\beta}\frac{\check{x}^2}{2}\right\} \quad (\check{x}\to\infty). \quad \text{(A 15}a\text{)}$$

Cavity region (cf. (3.9b)):

$$\bar{p}_0 \approx \bar{A}_0\left\{\epsilon^\beta\ln\left(\frac{1}{\epsilon}\right)(1-\beta)\,h\vartheta_0(\hat{H})\,(1-\tfrac{1}{2}\bar{x}^2)+\bar{x}-\tfrac{1}{6}\bar{x}^3\right\} \quad (\bar{x}\to 0). \quad \text{(A 15}b\text{)}$$

The only necessary comment on the above relations concerns the location at which the forcing given by (2.1) is brought in: as it is a wave reflected from the baffle and does not converge onto the slits, it is convenient to bring it into the matching procedure at the 'interface' between the neck region and the outside intermediate region, i.e. in (A 13a). The formal matching of the above four pairs of solutions is now straightforward. For the sake of brevity it is omitted, and only the results are given below:

$$\left.\begin{aligned}
&\hat{A}_0 = -\frac{i\pi}{2\epsilon^\beta\check{s}}\check{A}_0^{(0)},\\
&\check{B}_0^{(0)} = \check{A}_0^{(0)}\left\{\ln 2-\frac{i\pi}{2\epsilon^\beta\check{s}}\right\}, \quad \check{A}_0^{(0)} = -\tilde{A}_0,\\
&\tilde{B}_0 = \hat{p}_1+\tilde{A}_0\left\{(1-\beta)\ln\frac{1}{\epsilon}-\ln\frac{\pi}{\check{s}}+\mathbb{D}+\epsilon^{2\beta}\frac{\zeta(3)}{2}\left(\frac{\check{s}}{\pi}\right)^2\right.\\
&\qquad\left.+\epsilon^{2-2\beta}\frac{1+k^2}{3D^2}\left(\frac{\pi}{2\check{s}}\right)^2+\frac{i\pi}{2\epsilon^\beta\check{s}}+O(\epsilon^{4\beta},\epsilon^2,\epsilon^{4-4\beta})\right\},\\
&\bar{A}_0 = \check{A}_0^{(i)}\frac{\pi}{2\epsilon^\beta\check{s}},\\
&\check{B}_0^{(i)} = \check{A}_0^{(i)}\left\{\ln\left(\frac{1}{\epsilon}\right)\frac{\pi(1-\beta)\,h\vartheta_0(\hat{H})}{2\check{s}}+\ln 2\right\}, \quad \check{A}_0^{(i)} = \tilde{A}_0;
\end{aligned}\right\} \quad \text{(A 16)}$$

$$\left.\begin{aligned}
\frac{\hat{p}_1}{\tilde{A}_0} = 2\left\{(1-\beta)\ln\left(\frac{1}{\epsilon}\right)\left(\frac{\pi h\vartheta_0(\hat{H})}{4\check{s}}-1\right)\right.\\
\left.+\ln\frac{\pi}{\check{s}}-\mathbb{D}-\epsilon^{2\beta}\frac{\zeta(3)\,\check{s}^2}{2\pi^2}-\epsilon^{2-2\beta}\frac{1+k^2}{3D^2}\left(\frac{\pi}{2\check{s}}\right)^2-\frac{i\pi}{4\epsilon^\beta\check{s}}+O(\epsilon^{4\beta},\epsilon^2,\epsilon^{4-4\beta})\right\}.
\end{aligned}\right\} \quad \text{(A 17)}$$

REFERENCES

Gradshteyn, I. S. & Ryzhik, I. M. 1965 *Tables of Integrals, Series and Products.* Academic.

Kevorkian, J. & Cole, J. D. 1981 *Perturbation Methods in Applied Mathematics.* Springer.

Lamb, H. 1945 *Hydrodynamics.* Dover.

Monkewitz, P. A. & Nguyen-Vo, N.-M. 1985 The response of Helmholtz resonators to external excitation. Part 1. Single resonators. *J. Fluid Mech.* **151**, 477–497.

Morse, P. M. & Ingard, K. U. 1968 *Theoretical Acoustics.* McGraw-Hill.

Panton, R. L. & Miller, J. M. 1975 *J. Acoust. Soc. Am.* **57**, 1533–1535.

Smits, J. M. A. & Kosten, C. W. 1951 Sound absorption by slit resonators. *Acustica* **1**, 114–122.